Using Unsupervised Machine Learning for Plasma Etching Endpoint Detection

Imen Chakroun[1], Thomas J. Ashby[1], Sayantan Das[2], Sandip Halder[2], Roel Wuyts[1] and Wilfried Verachtert[1]

[1]*Exascience Life Lab, IMEC, Leuven, Belgium*

[2]*Advanced patterning, IMEC, Leuven, Belgium*

Keywords: Plasma Etch, Endpoint Detection, Principal Component Analysis, Clustering Algorithms.

Abstract: Much has been discussed around the advent of Industry 4.0 tools to improve yield across front-end and back-end semiconductor manufacturers. One of these tools is the etch endpoint detection (EPD) systems. It is essential to optimize the etch process by precisely landing on the underlying layers, because over-etching can cause underlying layer damage. In this work, we explore unsupervised machine learning for automatically identifying the endpoint during plasma etching of low open-area wafers using optical emission spectroscopy.

1 INTRODUCTION

Traditionally, the main driving force for the semiconductor industry is the continuous shrinking of device feature sizes, thereby incorporating more devices per unit area, reducing manufacturing cost and enhancing performance. However, the shrinking of feature size leads to a decrease in the process window imposing extremely tight requirement not only for the critical dimension (CD), but also for the edge and width roughness of spaces and trenches, of contacts and lines and 0f tip to tip (T2T) values. At sub-10nm technology nodes these parameters have significant influence on the overall device performance. It has been seen that CD and edge and width roughness and T2T values are highly influenced by the plasma etching process. After the lithography process, the target material to etch from the wafer surface reacts selectively with the plasma without affecting the underlying layers. Excess over etching can cause underlying layer damage, CD variations and influence the roughness if lines/trenches, resulting in yield loss. Thus, it is essential to optimize the etch process by precisely landing on the underlying layers. EndPoint Detection (EPD) is a technique that can help here.

During the plasma etch process specific gases are pumped into a chamber where they are turned into plasma by means of microwaves. The resulting plasma interacts with the exposed surface of the wafer in a highly controlled fashion. As said, it is critical to avoid excessive over-etching because it can damage the underlying layers causing device failures and subsequent yield reduction. As a mean to control the process, etch endpoint detection (EPD) has received great attention (H. Noh and Han., 2015) (H. Henry Yue and Toprac.,). The most widely used method for endpoint detection is to monitor the optical emission trace of reactive gases in the plasma using optical emission spectroscopy (OES) (Chen, 1996) (Puggini, 2015). OES is popular because OES measurements can be collected non-intrusively during wafer processing and because they provide real-time plasma chemical information, making them more reliable. The measurements correspond to the variation of the optical emission intensity of the plasma as a function of the reactants and by-products inside the etch chamber. Using this method, the endpoint is identified by monitoring the intensity of an emission peak corresponding

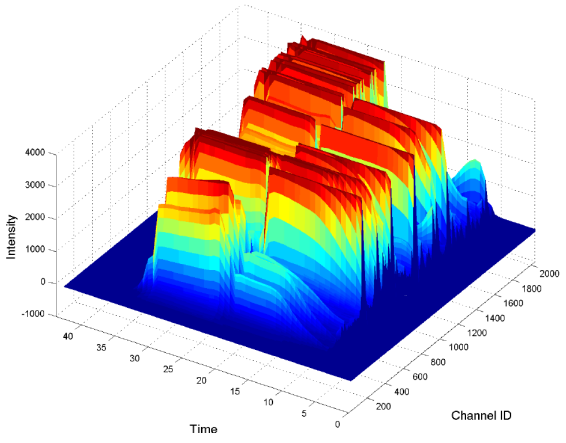

Figure 1: Mutliwavelength Optical Emission Spectra during main etch of oxide experiments.

to a particular reactant or product that show a pronounced variation at a certain time. However, using few manually selected wavelengths as an endpoint detection technique is only appropriate for high open areas. For low open area etches, tracking individual wavelengths often yields to an insufficient signal-to noise ratio (SNR). In small sample areas, changes in the optical signal are very small making it difficult to detect the etching endpoint. Moreover, if the viewport for optical-emission monitoring becomes blurred due to prolonged use of the etching system, optical-emission monitoring becomes impossible and regular maintenance of these observation windows is required (H. Jang and Chae., 2017). Other classical methods simply time the etch. In this case the resulting EPD is only valid for a very short number of runs before process drift and noise render the results ineffective.

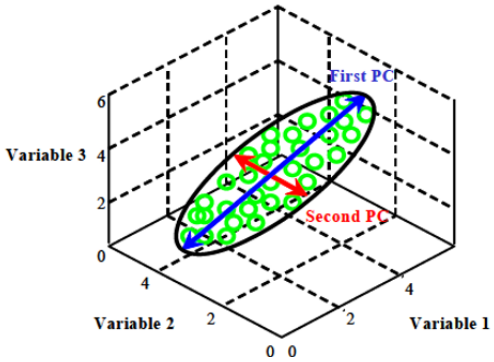

Figure 2: Principal component model of three dimensional data set lying primarily in a single plane. (Barry M. Wise, et al., 1996).

In this work, high-resolution multi-wavelength OES data is used to provide the necessary sensitivity for detecting subtle endpoint signals. Detecting etch endpoint from multi-wavelength OES data using existing simple methods is challenging. This is because these simple methods usually rely on finding a representative wavelength for each gas and each material used. Moreover, multi-wavelength OES data is high-dimensional and large, since it encapsulates measurements as a function of wavelength, time and intensity. Figure 1 plots a sample of 1200 spectral channels from 200 to 2000nm.

To overcome these challenges, data analysis techniques have been applied for etching processes (Puggini, 2015) (Goodlin, 2002). In this work, we combine feature extraction with unsupervised machine learning to extract key components that capture the endpoint signal. We first apply Principal Component Analysis (PCA) to the raw data. PCA uses an orthogonal transformation to convert a set of correlated variables into a new set of linearly uncorrelated variables called principal components. It's often used

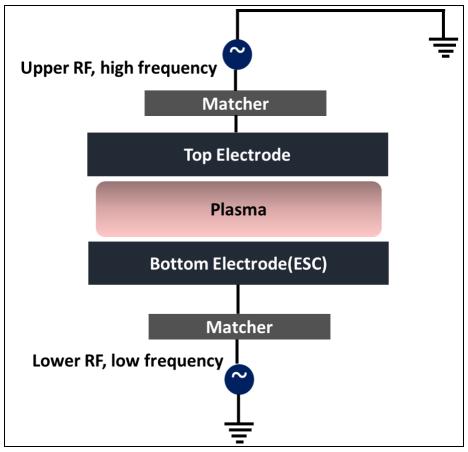

Figure 3: Schematic of a plasma etch chamber.

as a data compression algorithm or feature extraction technique. Therefore, we believe that PCA is suitable for extract small partial signal changes of multivariate signals as demonstrated in (H. L. Maynard and Ibbotson, 1996; S. Hong and Park, 2003). Afterwards, unsupervised clustering techniques such as the balanced iterative reducing and clustering using hierarchies algorithm (BIRCH) (Tian Zhang and Livny., 1997) are applied. The remainder of the paper is organized as follows: in Section 2 an overview of existing research work using machine learning techniques for EPD is given. In Section 3, our approach for EPD using unsupervised machine learning technique is presented. Experimental settings and results are described in Section 4. In Section 5, we provide a summary of the work and possible future research.

2 RELATED WORK

PCA has been suggested as a method for analyzing optical emission spectra due to its ability to dramatically reduce the dimensionality of large amounts of OES data. For example, Rangan et al (S. Rangan and Poolla, 1997) used PCA-reduced OES data to form a linear dynamical model capable of detecting endpoints and transition times in plasma etch. (A. d'Aspremont and Lanckriet, 2007) used sparse PCA for selecting key wavelengths from OES data. In (Goodlin, 2002), the authors reviewed statistical methods for OES in endpoint detection and suggested a novel method for weighting OES according to SNR. In (Han et al., 2008), the PCA algorithm was modified to determine the loading vector from the model wafer, and the score vector from the real-time data of the target wafer to reduce the processing time.

Due to their ability to synthesize nonlinear re-

lationships from process data, artificial neural networks found application in the prediction of etch endpoint detection (H. L. Maynard and Ibbotson, 1996). (S. Hong and Park, 2003) compared the use of PCA and ANNs for feature extraction from OES data and proposed a further ANN model for the reduced data. Similarly, (Kim and Kim., 2004) compared ANN and PCA but reported a significant performance improvement with partial OES models compared to conventional PCA-reduction. Other supervised machine learning techniques such as support vector machines (SVM) have been used in (K. Han and Chae.,) for endpoint detection based on OES measurement. In (H. Jang and Chae., 2017), analyzing the optical emission spectra with a K-means clustering algorithm is proposed on raw data.

In the next section we will explain how our proposed technique improves on the related work presented here.

3 ENDPOINT DETECTION USING PCA AND CLUSTERING

In this section we document the two main steps of our method, namely *i)* PCA for dimensionality reduction and variable selection, and *ii)* BIRCH clustering.

3.1 Dimensionality Reduction and Variable Selection

OES data are difficult to deal with since the number of variables (wavelengths) is usually larger than the number of measurements. In such cases, each variable can be obtained as a linear combination of the others making uncovering the true relationship between the different variables difficult. Principal component analysis (PCA) is a good candidate technique for dealing with such data being an established statistical method for multivariate data compression and information extraction. Its basic idea is to extract combinations of variables or factors (commonly expressed in percentage of explained variance) capable of reconstructing the majority of the information of the original high dimensional data. The concept of principal components is shown graphically in Figure 2 showing a three dimensional data set where the data lie primarily in a plane. The dimension reduction is achieved by identifying the principal directions, called principal components, in which the data varies. PCA assumes that the directions with the largest variances are the most "important". In this example, the first PC aligns with the greatest variation in the data. The second PC axis is the second most important direction and it is orthogonal to the first PC axis.

3.2 Clustering Techniques for Endpoint Detection

Etch endpoint detection is an unsupervised problem since no real ground truth can be used to control the data analysis technique. In production, EPD is based on best practices and domain expertise. Recall also that the basic idea of EPD is to find a change point or variation in the OES spectra that may alert about etch rate limit. This means we are looking for two disjoint group of points in the spectral curve that are separated by a change in the signal that define the before-endpoint and after-endpoint status. Hence, the idea of using unsupervised machine learning algorithms such as clustering which is the process of gathering objects in groups called clusters without prior knowledge only based on their similarity between each other and difference with objects from other groups. (H. Jang and Chae., 2017) also used clustering techniques for enhancing sensitivity of dielectric plasma etching EPD. In their case, K-means was applied on raw normalized data. In this work, hierarchical clustering is used via the balanced iterative reducing and clustering using hierarchies (BIRCH) algorithm with PCA as a dimensionality reduction technique. Using K-means cluster in real-time application is tricky because the load applied to the processor increases with continuous data collection and normalization of the optical signals. Moreover, K-means is very sensitive to noise and outliers since a small number of such data can substantially influence the centroids. BIRCH is an online-learning clustering algorithm, it's an incremental method that does not require the whole data set in advance. It is also local where each clustering decision is made without scanning all data points and currently existing clusters. It does not inspect all data points or all currently existing clusters equally for each 'clustering decision' and performs heuristic weighting based on the distance between these data points (Tian Zhang and Livny., 1997).

As aforementioned, the aim here is to construct two disjoint group of points representing the before and after etch endpoint. To construct such clusters, the OES data is split in batches that are normalized. PCA is applied and the output is fed to the birch algorithm. The resulting clusters are then evaluated using the silhouette score. The silhouette score (Rousseeuw, 1987) refers to a method of interpretation and validation of consistency within clusters of data, it measures the cohesion of the cluster (how similar an object is to its own cluster) and the separation compared to other

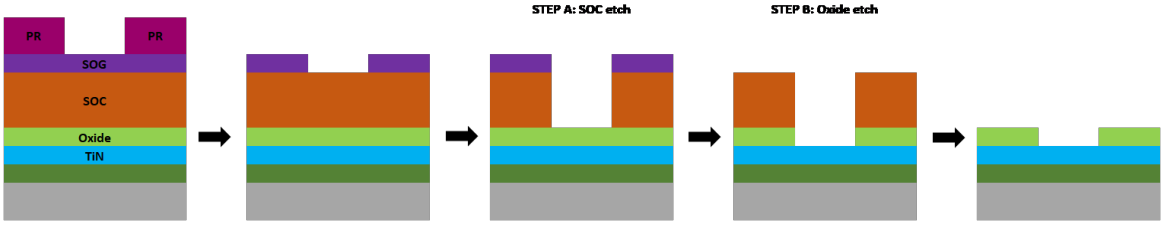

Figure 4: Simplified process flow for the etch process.

clusters. The silhouette ranges from -1 to 1 where coefficient values near 1 indicate that the sample is far away from the neighboring clusters, values of 0 indicate that the sample is on or very close to the decision boundary between two neighboring clusters and negative values indicate that those samples might have been assigned to the wrong cluster.

4 EXPERIMENTS

4.1 Experimental Settings

Etch Process: In Reactive-Ion Etching (REI), a high frequency electromagnetic field (HF) is applied to the upper electrode and low frequency field (LF) to the bottom electrode. The schematic of a plasma etch chamber is shown in Figure 3. During the plasma etch process the wafer is positioned on the bottom electrode and is held firmly in place by electrostatic chuck (ESC). The LF power applied to the bottom electrode determines the ion energy directing positive ions in the plasma onto the wafer and is responsible for physical etching. On the other hand, the HF applied to the top electrode influences the plasma density and is responsible for generating radicals for chemical etching.

In a production process, wafers are grouped in lots and processed sequentially undergoing several etching steps. Lots are also processed sequentially through etch chambers, interspersed with cleaning and maintenance operations. Cleaning cycles are typically done between each lot to remove the by-products of plasma etching that build up on the chamber walls, and are detrimental to etching performance.

Creation and Collection of Data: In major spectrometers, several channels are used each one recording a single wavelength. Wavelength intensity measurements are taken without interruption with a fixed sampling rate during processing of wafers. The resulting dataset is for every etching step a chronologically ordered values for a set of wafers. In this work, 21 wafers have been used. The wavelength intensities were measured during 500 to 1100 seconds at a sampling rate of 1 second using 1200 channels. For easy reading, the presented results are for one wafer.

A simplified process flow for the etch process is illustrated in Figure 4. In this study our focus will be on two steps in this process. For the remaining of the paper, we call Step A for the SOC etch step and Step B for the Oxide etch step.

4.2 Experimental Results

In Figures 5a and 6a, we plot the time series behavior of a sample OES spectrum for the wafer under investigation and the two etching steps A and B. It's clear from the figure that due to the big range of wavelengths, manually checking the variations in the signals is difficult or impossible. Thinking of selecting some dominant wavelengths based on domain knowledge is also misleading and incomplete. As an example, in Figures 5b and 6b four dominant spectral channels for the two aforementioned steps are plotted. For step B, in Figure 6b, the raw signal is almost uniform for three of the selected wavelengths and smoothly decreases over time for the 387nm wavelength. No distinct change point can be detected manually. However, in Figure 5b, one first big slope can be noticed around 30 seconds and a second smoother change can be seen between 70 and 90 seconds.

We applied first PCA to this dataset formatted as an $T \times W$ matrix, where T is the number of experimental runs and W is the number of measurements collected for each wavelengths. For every etching step a different matrix is considered. The results obtained by applying PCA to the complete OES spectrum presented in Figures 5a and 6a are plotted in Figures 7a and 7b respectively. In both plotted PCA first components, we can clearly identify two big variations in the signal: for Step A, in Figure 7a, in the interval [20 seconds,40 seconds]. For Step B, in Figure 7b, a big variations is observed between 50 and 65 seconds and a slighter one in the interval [25 seconds,35 seconds]. Compared to the original multi-wavelength signal, the new representation simplifies and condenses the data while keeping the same amount of information. Indeed, we report in Table

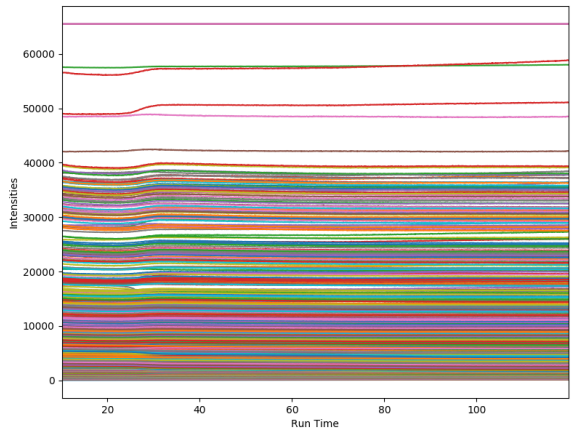

(a) Optical Emission Spectra during oxide etching experiments.

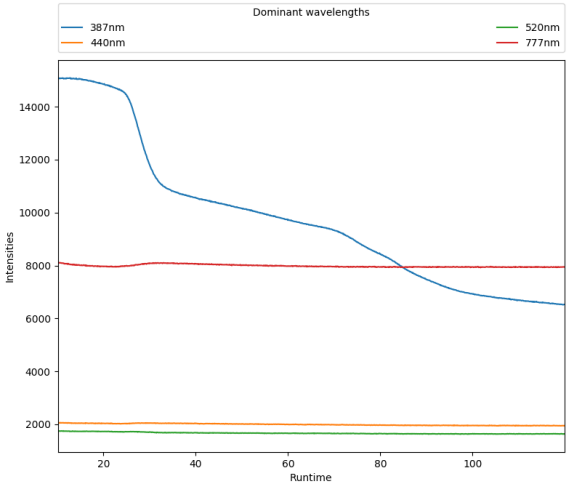

(b) Time series behavior of the selected dominant spectral channels.

Figure 5: Step A.

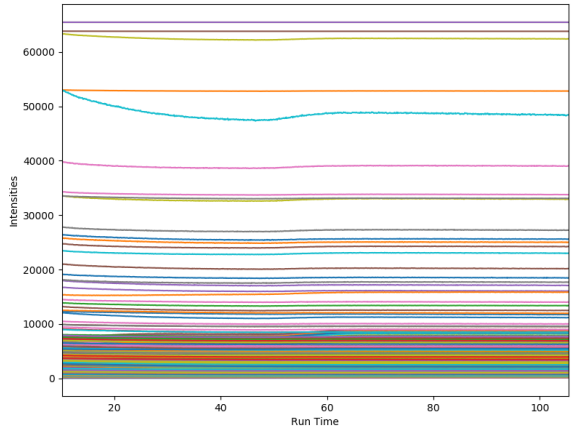

(a) Optical Emission Spectra during oxide etching experiments.

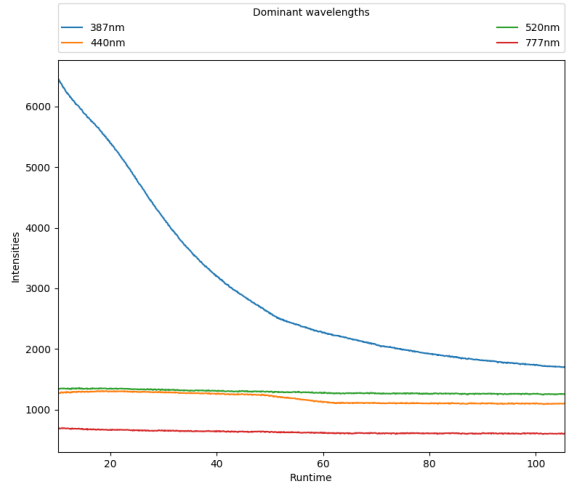

(b) Time series behavior of the selected dominant spectral channels.

Figure 6: Step B.

1 some of the explained variance randomly selected from the experimented wafers. On average, the percentage of variance explained by the first component is 0.913 for step A and 0.936 for step B.

In Figures 8a and 8b, we plot the silhouette score computed on the output of the clustering algorithm for step A and B respectively. As already explained, the silhouette score reflects the cohesion inside the cluster and the separation with other clusters. For Step A, in Figure 8a, the silhouette reaches a maximum value of 0.79 around 45 seconds and strongly decreases few seconds later around 57 seconds. For the rest of the runtime the values are roughly constant around 0.62. The peak value of the silhouette score at 45 seconds indicates that the data can be separated at that time and this separation can be defined as the etching endpoint. In Figure 8b, the silhouette score is plotted for step B. A first flat interval is observed around 45 seconds, a maximum value is reached afterwards around 70 seconds. The values are constants around 0.6 for the rest of the experiment. We suspect the endpoint here to happen around the 70 seconds which corresponds to the maximum value of the silhouette score.

(a) Step A

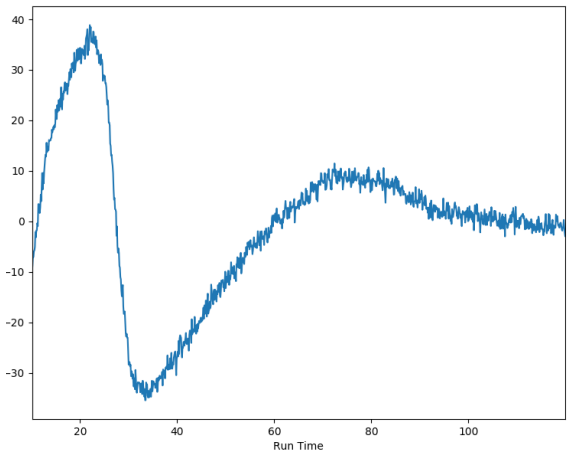

(b) Step B

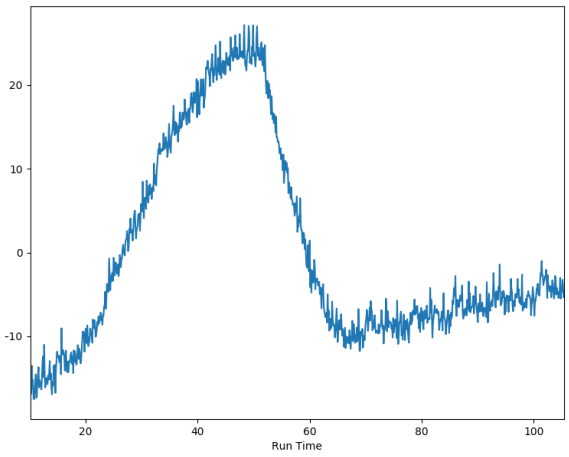

Figure 7: Plotting PCA first component.

(a) Step A

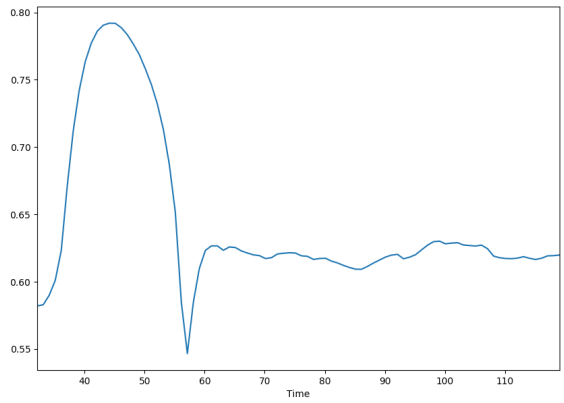

(b) Step B

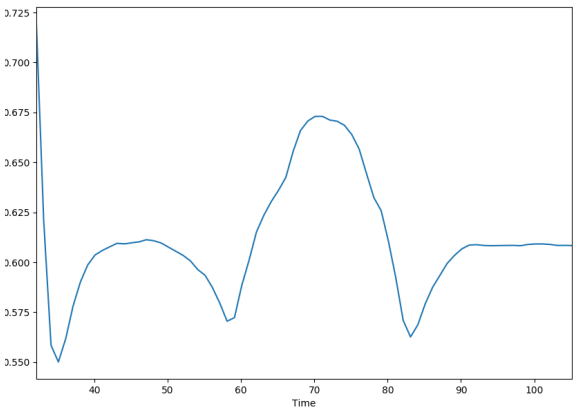

Figure 8: Silhouette score computed for the birch algorithm.

Table 1: Explained variances after PCA for randomly selected wafers.

Wafer	Explained variance Step A	Explained variance Step B
1	0.943	0.903
2	0.914	0.927
3	0.905	0.941
4	0.904	0.945
5	0.9027	0.950
6	0.908	0.950

5 CONCLUSION

In this work, we applied unsupervised machine learning techniques for identifying etch endpoint detection using high-resolution multi-wavelength OES data. PCA is first applied on the raw data to extract meaningful variables. Afterwards, the birch clustering is used to separate the data divided into batches in two clusters corresponding to the before-EPD and after-EPD. Satisfactory decision about etch endpoint were possible based on clearer variations in the silhouette score which was used as a metric for cluster separation. As further improvement of this work, we should be looking into methods that can produce the correct response even when the input data is corrupted by noise.

ACKNOWLEDGEMENT

This project has received funding from the Electronic Component Systems for European Leadership Joint Undertaking under grant agreement No 826589. This Joint Undertaking receives support from the European Unions Horizon 2020 research and innovation program and Netherlands, France, Italy, Belgium, Germany, Austria, Hungary and Israel.

REFERENCES

A. d'Aspremont, L. E. Ghaoui, M. J. and Lanckriet, G. R. G. (2007). A direct formulation for sparse pca using semidefinite programming. In *SIAM Rev.*, volume 49 no 3, page 434–448.

Chen, R., H. H. S. C. G. M. (1996). Plasma etch modeling using optical emission spectroscopy. *Journal of Vacuum Science & Technology*, 14:1901–1906.

Goodlin, B. E. (April 2002). *Multivariate endpoint detection of plasma etching processes*. PhD thesis, Univ. of Texas, Austin.

H. Henry Yue, S. Joe Qin, J. W. and Toprac., A. Plasma etching endpoint detection using multiple wavelengths for small open-area wafers.

H. Jang, H. Lee, H. L. C. K. and Chae., H. (February 2017). Sensitivity enhancement of dielectric plasma etching endpoint detection by optical emission spectra with modified k-means cluster analysis. In *IEEE Transactions on Semiconductor Manufacturing*, volume 30. issue 1.

H. L. Maynard, E. A. Rietman, J. T. C. L. and Ibbotson, D. E. (1996). Plasma etching endpointing by monitoring radio-frequency power In *Journal of Electrochem. Society*, volume 143 no 6, pages 2029–2035.

H. Noh, D. K. and Han., S. (2015). Real time endpoint detection in plasma etching using real-time decision making algorithm. In *China Semiconductor Technology International Conference, Shangai.*, pages 1–3.

Han, K., Yoon, E. S., Lee, J., Chae, H., Han, K. H., and Park, K. J. (2008). Real-time end-point detection using modified principal component analysis for small open area sio2 plasma etching. In *Industrial & Engineering Chemistry Research*, volume 47, no 11, pages 3907–3911.

K. Han, S. Kim, K. J. P. E. S. Y. and Chae., H. Principal component analysis based support vector machine for the endpoint detection of the metal etch process. In *Proc. IFAC World Congr.*

Kim, B. and Kim., S. (2004). Partial diagnostic data to plasma etch modeling using neural network. In *Microelectron. Eng.*, volume 75 no 4, pages 397–404.

Puggini, L., M. S. (2015). Extreme learning machines for virtual metrology and etch rate prediction. In *26th IEEE Irish Signals and Systems Conference (ISSC)*, pages 1–6.

Rousseeuw, P. J. (1987). Silhouettes: A graphical aid to the interpretation and validation of cluster analysis. In *Journal of Computational and Applied Mathematics*, volume 20, pages 53–65.

S. Hong, G. M. and Park, D.-C. (2003). Neural network modeling of reactive ion etching using optical emission spectroscopy data. In *IEEE Trans. Semicond. Manuf.*, volume 16 no 4, pages 598–6081–6.

S. Rangan, C. S. and Poolla, K. (1997). Modeling and filtering of optical emission spectroscopy data for plasma etching systems. In *IEEE International Symposium of Semiconducter Manufacturing*, page B41–B44.

Tian Zhang, R. R. and Livny., M. (January 1997). Birch: A new data clustering algorithm and its applications. In *Data Min. Knowl. Discov.*, pages 141–182.